Extremophiles (2007) 11:179–189
DOI 10.1007/s00792-006-0030-5

ORIGINAL PAPER

Sara Lawrence Powers · Clifford R. Robinson
Anne Skaja Robinson

Denaturation of an extremely stable hyperthermophilic protein occurs via a dimeric intermediate

Received: 6 May 2006 / Accepted: 4 August 2006 / Published online: 28 October 2006

Abstract To elucidate determinants of thermostability and folding pathways of the intrinsically stable proteins from extremophilic organisms, we are studying β-glucosidase from *Pyrococcus furiosus*. Using fluorescence and circular dichroism spectroscopy, we have characterized the thermostability of β-glucosidase at 90°C, the lowest temperature where full unfolding is achieved with urea. The chemical denaturation profile reveals that this homotetrameric protein unfolds at 90°C with an overall ΔG° of $\sim$ 20 kcal mol^{-1}. The high temperatures needed to chemically denature *P. furiosus* β-glucosidase and the large ΔG° of unfolding at high temperatures shows this to be one of the most stable proteins yet characterized. Unfolding proceeds via a three-state pathway that includes a stable intermediate species. Stability of the native and intermediate forms is concentration dependent, and we have identified a dimeric assembly intermediate using high temperature native gel electrophoresis. Based on this data, we have developed a model for the denaturation of β-glucosidase in which the tetramer dissociates to partially folded dimers, followed by the coupled dissociation and denaturation of the dimers to unfolded monomers. The extremely high stability is thus derived from a combination of oligomeric interactions and subunit folding.

Keywords Archaea · Hyperthermophile · Determinants of stability · Oligomerization · Tetramer · β-Glucosidase · *Pyrococcus furiosus* · CelB

Communicated by A. Driessen.

S. L. Powers · A. S. Robinson (✉)
Department of Chemical Engineering, University of Delaware, Newark, DE 19716, USA
E-mail: robinson@che.udel.edu
Tel.: +1-302-8310557
Fax: +1-302-8311048

C. R. Robinson
Department of Chemistry and Biochemistry, University of Delaware, Newark, DE 19716, USA

Abbreviations GdnHCl: Guanidine hydrochloride · CD: Circular dichroism

Introduction

In the past, the inability of enzymes to retain structure and function outside a narrow range of conditions—centered around room temperature, atmospheric pressure, neutral pH, and low salinity—restricted their use as biocatalysts. The limits of protein stability defined the boundaries of how enzymes could be effectively used in applications such as food processing, pulp and paper manufacturing, bioremediation, and specialty chemical and detergent production (Grimsley et al. 1997; Bauer et al. 1998; Wallecha and Mishra 2003). Since the discovery over the past 30 years of microorganisms inhabiting some of the harshest ecosystems known on Earth, this view has changed; nature has already engineered enzymes that catalyze reactions under extreme conditions (Adams and Kelly 1998; Demirjian et al. 2001).

We are studying the thermostability of a homo-tetrameric β-glucosidase from the Archaeon *Pyrococcus furiosus*, an organism with optimal growth around 100°C (Fiala 1986). As Pyrococcal β-glucosidase does not unfold even at 100°C, it represents a good model for additional studies of extreme protein stability; β-glucosidases are also well suited for such analysis, as members of this family span a wide range of temperatures (Voorhorst et al. 1995) and host organism systems (Bauer et al. 1996). Pyrococcal β-glucosidase has previously been shown to be a homo-tetramer; monomers have a MW = 56.4 kDa and there are two catalytic glutamate residues per subunit (Voorhorst et al. 1995). Subunits are arranged in a $(\beta\alpha)_8$-barrel fold similar to other family members (Kaper et al. 2000). Pyrococcal β-glucosidase was chosen because it is an industrially relevant biocatalyst in the family 1 glycosyl hydrolases (Bauer et al. 1998), it is the most thermostable and thermoactive member of its family (Kengen et al. 1993;

Kaper et al. 2000), an expression system was previously established (Smith and Robinson 2002), and denaturation can be monitored by fluorescence and circular dichroism (CD) spectroscopy. A 3.3 Å X-ray structural model is available (S.J.J. Brouns, T. Kaper, W.M. de Vos and J. van der Oost, unpublished data).

Here, we characterize the stability and denaturation profile of *β*-glucosidase, using fluorescence and CD spectroscopy to monitor chemically induced denaturation. Because urea denaturation cannot be achieved at room temperature, denaturation experiments were conducted at 90°C where this protein is still fully folded and active. In contrast, many mesophilic, and even many thermophilic proteins, are denatured at 90°C even in the absence of chemical denaturants. We therefore find that *β*-glucosidase is remarkably stable, with a free energy of denaturation around 20 kcal mol^{-1} at 90°C. Analysis of the concentration dependence of stability, in concert with high temperature native gel electrophoresis and Ferguson analysis, was used to show that unfolding occurs through a dimeric intermediate.

Results

Unfolding monitored by fluorescence spectroscopy

At 102–105°C, *P. furiosus β*-glucosidase has one of the highest reported temperatures of optimal activity for a hyperthermophilic enzyme (Kengen et al. 1993), and yet the full temperature profile of the free energy for unfolding could not be determined. At room temperature, urea does not denature the protein (data not shown), proving this protein is more stable at moderate temperatures than any protein where the ΔG° of unfolding can be determined with urea alone. Similarly, in the absence of urea and GdnHCl, the protein remains folded even at 90°C, as monitored by intrinsic tryptophan fluorescence; the spectral center of mass (Eq. 1; Materials and methods) at 25 and 90°C were equivalent (data not shown). A large decrease in intensity is seen upon raising the temperature, however, due to the intrinsic temperature dependence of the fluorescence emission. Increasing temperature in the absence of chemical denaturants induces irreversible aggregation at temperatures over approximately 105°C. Only a combination of 90°C and 7 M urea or 80°C and 5 M GdnHCl is sufficient to induce complete denaturation (Fig. 1a, b). At these conditions, a red shift in the center of mass from around 340 to 353 nm with a large drop in fluorescence intensity is induced. The intrinsic decrease in fluorescence quantum yield at high temperatures places a lower practical limit on the concentration of protein we can use in the fluorescence experiments, and decreases the signal-to-noise ratio. Denaturation with GdnHCl could be fully completed at 80°C (Fig. 2a). While GdnHCl induced irreversible aggregation in the first transition from concentrations around 1.2–1.6 M, three-state behavior was seen in concentrations where no

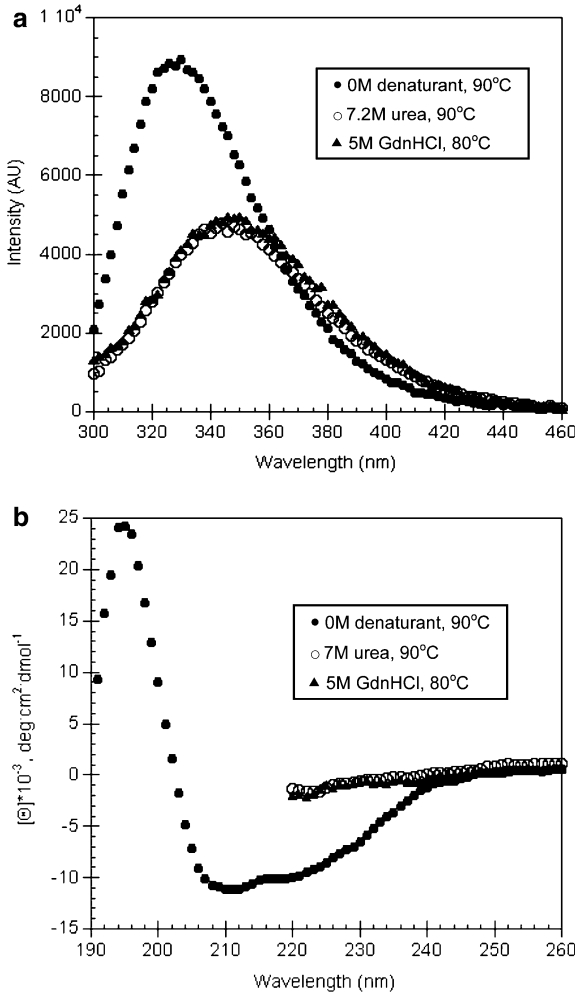

Fig. 1 Fluorescence and CD spectra of *P. furiosus β*-glucosidase at 1.84 μM. **a** Fluorescence emission spectra at 20 mM sodium phosphate buffer, pH 6.5, at 90°C and 0 M urea (*filled circles*, center of mass = 339.8 nm), at 90°C and 7.2 M urea (*open circles*, center of mass = 352.9 nm), and at 80°C and 5 M GdnHCl (*filled triangles*, center of mass = 353.2 nm). **b** CD spectra of native structure at 0 M denaturant (90°C) (*filled circles*) and denatured *β*-glucosidase in 7.2 M urea (90°C) and 5 M GdnHCl (80°C) (*open circles* and *filled diamonds*, respectively), in 20 mM sodium phosphate buffer (pH 6.5). Each spectrum represents an average of three scans, and buffer baseline is subtracted. The spectra for samples containing urea were taken from 260 to 220 nm, in the range where there is no interference from absorbance of urea

aggregation occurred. Aggregation was observed both visually and by a gradual decrease in the fluorescence emission monitored at 330 nm over time. The first transition was complete at around 2.2 M GdnHCl, with a spectral signal at the second plateau around 349 nm. The second transition was completed around 4 M GdnHCl with little change up to 5 M GdnHCl.

Since *P. furiosus β*-glucosidase is a homotetramer, we sought to understand whether one or both of the transitions involved subunit dissociation. We performed denaturation experiments at fivefold lower and fivefold higher protein concentrations to determine whether the transitions depended on the protein concentration, as

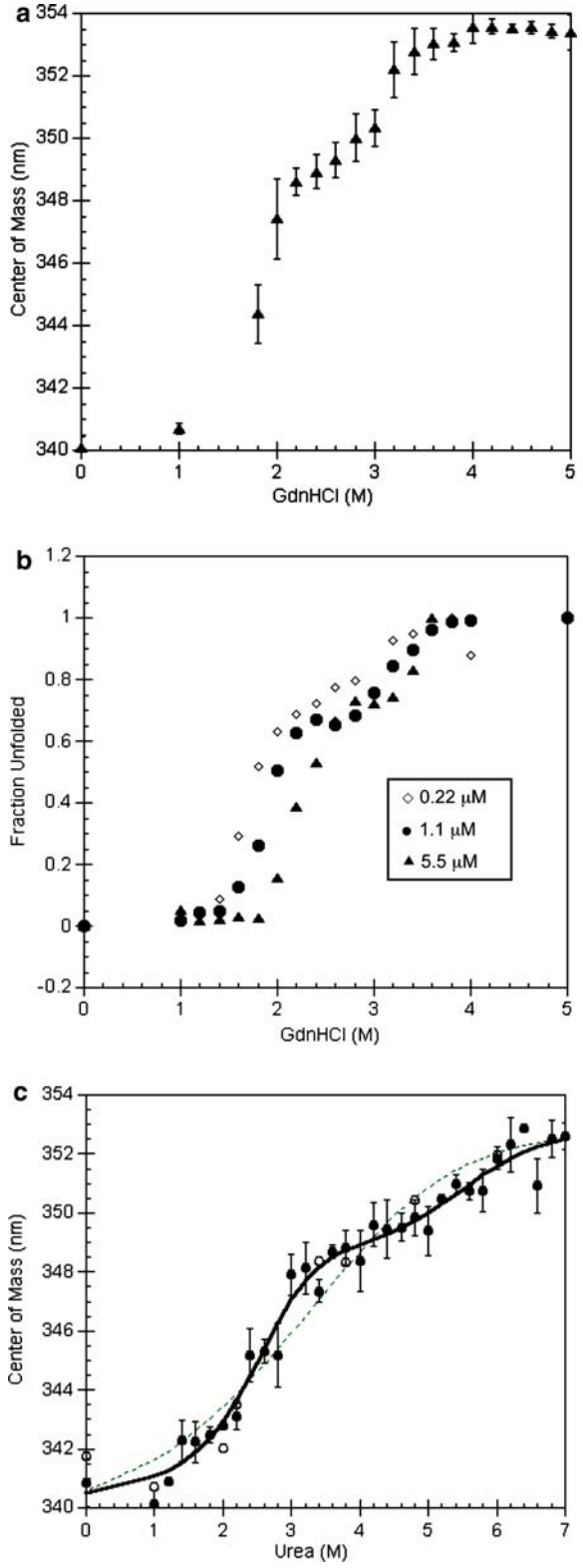

Fig. 2 **a** Denaturation profile of *β*-glucosidase at 1.84 μM as unfolded with GdnHCl (*filled triangles*). Points omitted in concentrations where GdnHCl induced aggregation (1.2–1.6 M). *Data points* indicate the center of mass. *Error bars* indicate one standard deviation of at least three replicates. **b** Fluorescence denaturation profiles of *β*-glucosidase at varying protein concentrations show both transitions are concentration dependent. *Data points* indicate the normalized center of mass of fluorescence emission spectra collected during denaturation with GdnHCl at 80°C using *β*-glucosidase concentrations of 0.22 μM (*open diamonds*), 1.1 μM (*filled circles*), and 5.5 μM (*filled triangles*). The 5.5 μM spans only to 3.6 M GdnHCl due to solubility limitations. **c** Urea denaturation profile of *β*-glucosidase at 1.84 μM (*filled circles*) monitoring fluorescence. The *solid line* represents the best nonlinear least squares fit to the three-state model $N_4 \leftrightarrow 2N_2 \leftrightarrow 4U$, using $\Delta G°$ of 5.7 kcal mol^{-1} for the first transition and 16.1 kcal mol^{-1} for the second transition. The *dashed line* represents a two-state non-linear least square curve fit corresponding to the model $N_4 \leftrightarrow 4U$. *Open circles* represent renaturation at 1.84 μM

such a dependence would indicate a change in oligomeric state for that transition (Timm and Neet 1992; Grimsley et al. 1997; Hobart et al. 2002) as described in the equilibrium model by Eq. 3 (Materials and methods). Both transitions appeared to be concentration dependent: at lower protein concentration, both transitions shift to lower GdnHCl concentrations; at higher protein concentrations, both transitions shift to higher GdnHCl concentrations (Fig. 2b). In all cases, the shapes of the denaturation profiles were unchanged. Thus, the stability of the native state and the intermediate state increases with increasing protein concentration, suggesting that both transitions involve a dissociation event.

Because of aggregation effects with GdnHCl and the need to determine the oligomeric state using the technique of native gel electrophoresis described in later sections, we also were interested in verifying the three-state denaturation with urea. Urea titration from 0 to 7 M indicates that denaturation did occur via a three-state process (Fig. 2c). The first transition occurs from about 1–3.6 M urea with a red shift in the center of mass from 340 to 349 nm. A plateau is observed from 3.6 to 5.2 M urea, with a change in the center of mass of only about 0.5 nm. The second transition occurs from 5.2 to 6.2 M urea where the center of mass shifts from 349 to 353 nm. An upper plateau is reached after 6.2 M, with very little change in the spectral signal occurring up to 7 M urea. Although we had concerns about carbamylation from cyanate formation of urea at high temperatures, each point of the fluorescence experiments was run independently to limit the exposure of samples to urea at high temperature, and the similar behavior observed with GdnHCl validates the observations. We also performed urea denaturation experiments at different protein concentrations. While the urea denaturation curves at 90°C were noisier than those of GdnHCl at 80°C due to the higher temperature and the decrease in intensity due to fluorescence emission temperature dependence, similar concentration dependence was seen for both transitions with urea (data not shown).

The urea denaturation profiles fit poorly to a two-state model, but fit quite well to a three-state model for unfolding (Fig. 2c). The sum of the square error between the fits and data was over twice as large for the two-state fit as the three-state fit (22.3 vs. 9.5, respectively). Urea

unfolding was essentially fully reversible, with little hysteresis observed (Fig. 2c, open symbols). Because at low concentrations GdnHCl denaturation induced aggregation and was not fully reversible, no thermodynamic parameters were determined.

Unfolding monitored by circular dichroism

As expected for a protein that contains significant α-helical structure, the CD spectrum of *P. furiosus* β-glucosidase at 90°C showed characteristic minima at 208 and 222 nm. Upon denaturation at 90°C and 7 M urea, most secondary structure was lost (Fig. 1b). To determine whether the intermediate species observed with fluorescence spectroscopy retained any secondary structure, a denaturation curve was constructed by monitoring the change in ellipticity at 225 nm (Fig. 3). Because of the high absorbance of urea at low wavelengths, the spectra for samples containing urea were taken from 260 to 220 nm, in the range where there is no interference from urea. While the plateau was not as pronounced as that observed by fluorescence spectroscopy, the broad denaturation curve could not be fit to a single transition. Therefore this denaturation profile was also fit with the three-state model. The center of the first transition monitored by CD (from 2.4 to 4.2 M urea) appears slightly shifted at around 3 M urea relative to the center of the first fluorescence transition at 2.5 M urea. The early part of the fluorescence transition is believed to be due to changes in quaternary and tertiary structure that would not be detected by circular dichroism spectroscopy at 225 nm. However, both CD and fluorescence curves show a plateau between 4 and 5 M urea; the second transition observed by CD (from 5.2 to 6.4 M urea) superimposes fairly well with the second fluorescence transition. The change in CD signal in the first transition was displaced from the corresponding shift in the fluorescence center of mass as denaturant concentration was increased, suggesting that the first transition involves relatively significant early changes in tertiary and/or quaternary structure that occur before changes in secondary structure are seen by circular dichroism.

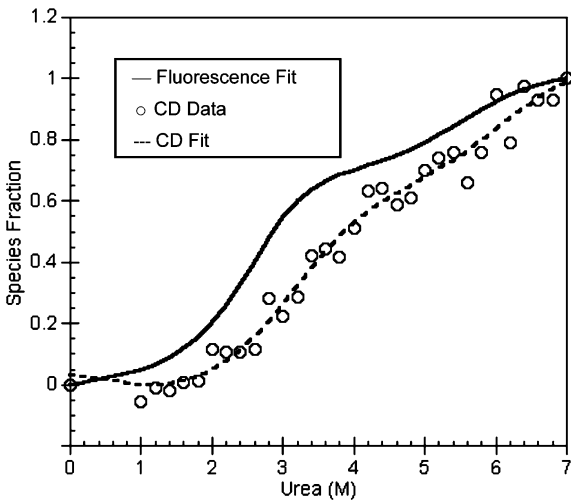

Fig. 3 Urea denaturation profile of β-glucosidase at 1.84 μM measured by circular dichroism spectroscopy. Each point represents an average of three measurements with buffer baseline subtracted (*open circles*). The *dashed line* represents the best nonlinear least squares fit to the three-state model $N_4 \leftrightarrow 2N_2 \leftrightarrow 4U$, using ΔG° of 4.0 kcal mol^{-1} for the first transition and 14.6 kcal mol^{-1} for the second transition. For comparison, the best fit to the fluorescence data (taken from Fig. 2) is shown as a *solid line*

Dimeric species is populated

Due to the concentration dependence of both unfolding transitions and the natural symmetry of this β-glucosidase (formed with two pairs of identical interfaces), the intermediate seen with fluorescence and CD spectroscopy was most likely dimeric. With this preliminary evidence, we sought to confirm the intermediate oligomeric state by a nonspectroscopic method. Because most other common biophysical methods are not practical or feasible at the high temperatures and urea concentrations necessary to denature β-glucosidase, we used high temperature gel electrophoresis and Ferguson analysis to detect the dimeric intermediate (Ferguson 1964; Hames 1990).

To capture all oligomeric states during denaturation, nondenaturing PAGE was carried out in the presence of 7 M urea under various denaturing conditions (±SDS, with and without preheating to 100°C) at 60°C. To limit the formation of cyanate from the decomposition of urea, which can react with the lysine and arginine residues or the N-terminus of the protein, an ion exchange resin, AG 501-X8 (Biorad, Hercules, CA, USA), was added to the heated solution. Under these varying conditions, we observe four species (Fig. 4a). Without pre-heating, a band corresponding to the tetramer is predominant; a higher molecular weight species is also present (Fig. 4a; lanes 1, 2). The predominant species was confirmed to be a tetramer by static light scattering at room temperature (not shown). When the samples are preheated to 100°C for 20 min in the presence of 7 M urea, the tetramer band disappears and two new bands with increased mobility are observed (lane 3). Addition of SDS increases the intensity of the fastest-running band (lane 4); this harsh combination of denaturants has been shown previously to yield a fully denatured monomeric species using SDS PAGE. SDS does not alter the mobility of the tetrameric species in native PAGE because it does not denature the protein and expose or bind to the hydrophobic core at low temperatures, but rather diffuses and migrates out of the sample during electrophoresis. The density of each of the four lanes was measured and compared using NIH Image Version 1.62 (Rasband, National Institute of Health) to ensure constant protein concentration in all four lanes, as lanes three and four were difficult to dis-

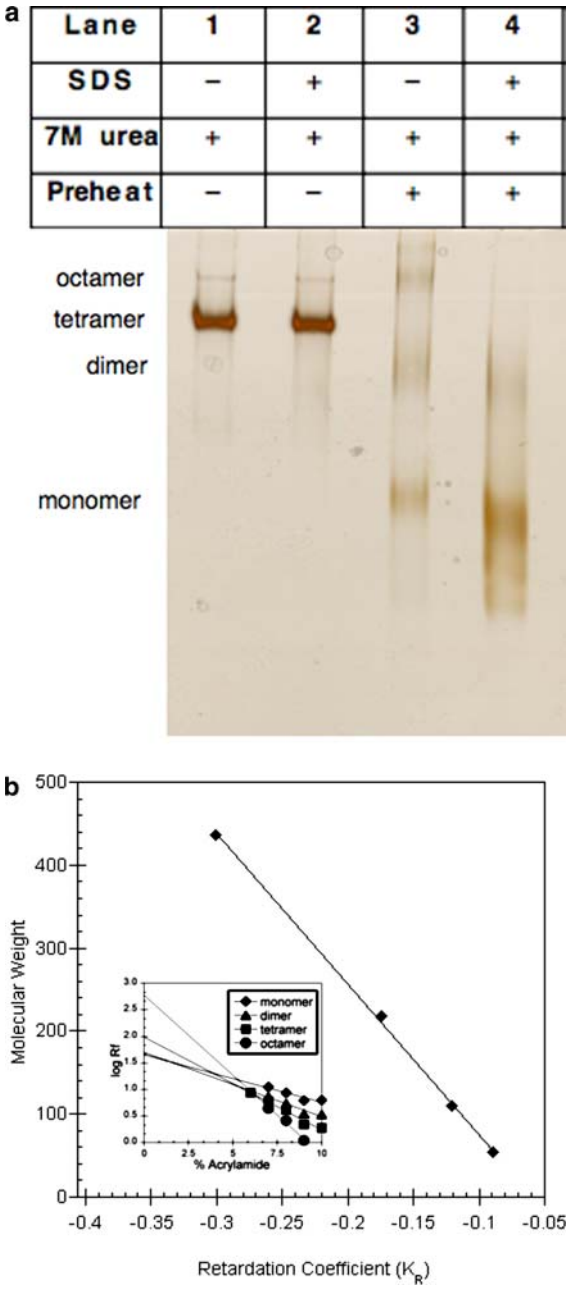

Fig. 4 Native gel electrophoresis and Ferguson analysis of *β*-glucosidase. **a** Native gel at 9% acrylamide run at 60°C. *Lane 1* *β*-glucosidase in 7 M urea, native sample buffer, unheated. *Lane 2* *β*-glucosidase in 7 M urea, SDS sample buffer, unheated. *Lane 3* *β*-glucosidase in 7 M urea, native sample buffer, preheated to 100°C for 15 min before loading. *Lane 4* *β*-glucosidase in 7 M urea, SDS sample buffer, preheated to 100°C for 15 min before loading. The identification of the four bands (''monomer'', ''dimer'', ''tetramer'', and ''octamer'') is based on the Ferguson analysis shown in part **b**. **b** Ferguson analysis of *P. furiosus* *β*-glucosidase. Relative retardation coefficient K_R (derived from the slope of the Ferguson plot in inset plot) are plotted versus molecular weight for each identified species. The *line* represents the best fit, assuming monomeric molecular weight = 56.4 kDa, dimer = 109.2 kDa, tetramer = 218.4 kDa, and octamer = 436.8 kDa. *Inset* Data points represent migration of monomer (*filled diamonds*), dimer (*open triangles*), tetramer (*filled squares*), and octamer (*open circles*). Log of retention factor, or distance migrated in gel (R_f) is plotted versus acrylamide concentration from each gel. Lines correspond to the best linear fit through the data

cern by eye due to band smearing. While lane three was seen to slightly decrease possibly due to loss of protein during heating/cooling as the protein was loaded onto the gel, the loss was slight and the total density of lane four was consistent with the first two lanes.

To confirm the identities of the oligomeric states, PAGE experiments were performed using acrylamide concentrations ranging from 6–10%. The mobilities of the four distinct species were measured and plotted versus acrylamide concentration (Fig. 4b, inset). A least-squares fit of the mobility data was performed, and the relative retardation coefficients (K_R) were calculated from the fitted slopes of these mobilities. The K_R values were then plotted as a function of the theoretical molecular weight of the monomeric, dimeric, and tetrameric species (Fig. 4b) as described previously (Hames 1990; Benton et al. 2002). The higher molecular weight species fit well to an octamer. The data from all four species agree very well with this model (Fig. 4b; $R^2 > 0.99$).

To show progression of unfolding from tetramer to dimer to monomer, samples were prepared in 4 M urea and run on PAGE with increasing concentrations of SDS (Fig. 5) (the octamer is not detected when urea is present and the sample is preheated to 100°C prior to electrophoresis). As SDS concentration increases, we observe conversion of *β*-glucosidase from tetramer to a mixture of tetramer and dimer, and eventually to a mixture of tetramer, dimer, and monomer. Evidence for protein modification due to cyanate formation by the presence of additional bands following denaturation at varying times of exposure to urea was not observed in our studies, by contrast to that described previously (Gerding et al. 1971). This suggests that under the time frame of our studies, no significant modification is occurring, consistent with the reversibility observed by intrinsic fluorescence.

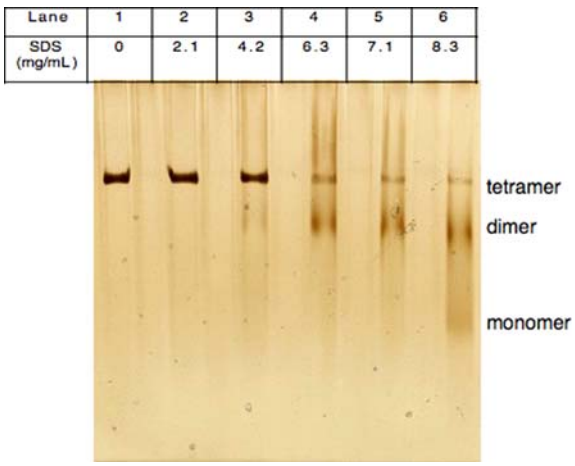

Fig. 5 Native gel at 9% acrylamide run at 60°C. *β*-Glucosidase samples in 4 M urea, preheated to 100°C. Concentration of SDS increases from left to right. Transition from tetramer with dimer and monomer is observed with increasing SDS concentrations

Although the conditions used in the electrophoresis experiments do not exactly correspond to the conditions used in the fluorescence and CD experiments (the maximum running temperature for the electrophoresis apparatus is 60°C), Ferguson analysis confirms that a dimeric form of β-glucosidase can be populated as a folding/assembly intermediate under moderately denaturing conditions, in agreement with the concentration dependence of β-glucosidase stability, and our model for the folding pathway.

Model for β-glucosidase unfolding

Based on the fluorescence, CD and native PAGE data, the intermediate formed during unfolding appears to be a dimer, in which some local unfolding has occurred but much of the native secondary structure remains intact. Such a model is consistent with the positions of the tryptophan residues; some secondary structure would have to be lost to expose these residues and cause a shift in the center of mass. This three-state model was used to estimate the free energies of unfolding, *m*-values, and the spectroscopic signal of a pure intermediate species for a three-state reaction ($\Delta G°_1$, m_1, $\Delta G°_2$, m_2, and Y_I).

Using the three-state model, the fractions of native, unfolded, and intermediate species were determined at all urea concentrations (Fig. 6). The dimeric intermediate species begins to appear even at 1 M urea and is the predominant form between 3 and 5 M urea.

The resulting thermodynamic parameters from the three-state fits of fluorescence and CD denaturation curves are reported in Table 1. The ΔG° and *m* values for both transitions determined by CD and fluorescence data agree well with each other. The free energy of unfolding for the first transition was 5.6 kcal mol^{-1} measured by fluorescence spectroscopy and 4.0 kcal mol^{-1} measured by CD; the *m* values were 2.3 and 3.2 kcal mol^{-1} M^{-1}, respectively. For the second transition, the free energy of unfolding was 16.1 kcal mol^{-1} by fluorescence spectroscopy and 14.6 kcal mol^{-1} by CD, and the *m* values were 1.2 and 2.7 kcal mol^{-1} M^{-1}, respectively.

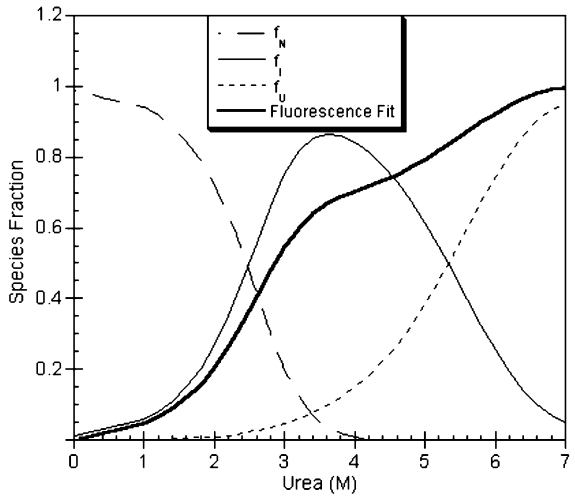

Fig. 6 Theoretical populations of each β-glucosidase species at increasing urea concentration. Populations of Native (f_N, *dashed line*), Intermediate (f_I, *thin solid line*), and Unfolded (f_U, *dotted line*) species, are based on parameters obtained from the fluorescence denaturation profile shown in Fig. 2c (90°C, pH 6.5, and 1.84 μM β-glucosidase). For comparison, the normalized three-state fit to the experimental fluorescence denaturation data is shown as *thick line*

Table 1 Comparison of thermodynamic parameters for denaturation using a three-state model

	Fluorescence (urea)	CD (urea)
M_1	2.3 ± 0.4	1.2 ± 0.3
M_2	3.2 ± 0.9	2.7 ± 1.4
$\Delta G°_1$ (kcal mol^{-1})	5.7 ± 1.0	4.0 ± 0.8
$\Delta G°_2$ (kcal mol^{-1})	16.1 ± 4.7	14.6 ± 8.6
$\Delta G°_{total}$ (kcal mol^{-1})	21.8	18.6

The error estimates represent a 95% confidence interval on the four parameters as described in Materials and methods

The center of mass of fluorescence emission for the intermediate species was best fit to approximately 349 nm, with an ellipticity of approximately, −4.8 mdeg. These fitted values differ somewhat from the magnitude of the signals in the plateau region because some native and unfolded species are present, even though the intermediate is predominant. About two-thirds of the total free energy is expended in the second transition, suggesting that the subunit interactions in the dimer and secondary and tertiary structure of the monomer provide most of the stabilizing energy. Additional evidence for this interpretation of the unfolding data of *P. furiosus* β-glucosidase is the similar distribution and unfolding pathway through a dimeric intermediate observed for a homologous (lower stability) tetrameric β-glycosidase from *Sulfolobus solfataricus* (Catanzano et al. 1998) as measured by size exclusion chromatography. Here we are unable to utilize chromatography due to the high temperatures needed to dissociate the *P. furiosus* β-glucosidase.

Activity assay in the presence of urea

We sought to determine a relationship between changes in the quaternary structure and the loss of enzymatic activity. Previous reports have suggested that *P. furiosus* β-glucosidase is active only in the tetrameric form (Pouwels et al. 2000). We measured enzymatic activity of β-glucosidase at 90°C with increasing urea concentrations. We found that the activity decreased by 88% in the range of urea concentrations that spanned the first denaturation transition (0–4 M urea) (not shown). However, we cannot unambiguously assign this loss of activity to dissociation. Control experiments show that urea alone decreases the amount of measured β-glucosidase activity by 80% at 30°C, where spectroscopic analyses indicate no dissociation or denaturation occurs

(not shown). Similarly, the activity decreased by 75% in the presence of 1M GdnHCl at 30°C. We believe that urea and GdnHCl interfere with the assay for reasons unrelated to β-glucosidase protein conformation.

Discussion

Pyrococcus furiosus β-glucosidase represents a new realm of protein stability. Most thermodynamic analyses of folding, even for extremophilic proteins, are performed on proteins that can be denatured by heat (T_m < 100°C), urea, or GdnHCl alone. *Pyrococcus furiosus* β-glucosidase is essentially fully folded at 100°C (as evidenced by circular dichroism) or in the presence of 7 M at room temperature. The overall ΔG° at 90°C is around 20 kcal mol^{-1} based on fluorescence and CD spectroscopy. Compared to a homologous protein from *S. solfataricus* that can be denatured with urea alone at 30°C with a similar pathway to *P. furiosus* β-glucosidase, the stability reported here is extraordinary. While we have not yet determined its exact stability at 25°C, it is presumably more stable at 25°C than at 90°C, based on the fact that at 25°C, 7 M urea does little to disrupt the protein structure.

Often it is difficult to determine the thermodynamic stability of hyperthermophilic proteins, but other proteins from *P. furiosus* have also been shown to be intrinsically very stable at high temperatures, such as an L-threonine dehydrogenase with increasing catalytic activity up to 100°C (Machielsen and van der Oost 2006), a ferritin with a half-life of 85 min at 120°C based on activity (Tatur et al. 2006), and an endo-β-1,3 glucanase that resisted conformational changes until incubation at 150°C (Koutsopoulos et al. 2005). However, physiological features of an organism can also have an effect, for example a small heat shock protein (sHSP) from *P. furiosus* that extrinsically increases the activity and stability of some proteins has been identified (Chen et al. 2006). These physiological conditions are important to consider; while the stability measured in in vitro experiments provides information about the molecule, it may not quantitatively reflect the in vivo stability. The thermostability of β-glucosidase at the optimal growth temperature of *P. furiosus* at around 100°C is likely to be lower than the 20 kcal mol^{-1} measured at 90°C. The in vitro stability is determined at specific buffer conditions and protein concentrations that do not imitate the in vivo environment. Different buffers have been shown to affect the stability of this β-glucosidase (Kengen et al. 1993). In addition, as this protein is oligomeric, lower total protein concentrations will destabilize the oligomeric form, favoring unfolding.

Although the native gels were not run strictly under the same conditions as the spectroscopic data due to instrument temperature limitations, we have shown that a dimeric intermediate is stable under moderately denaturing conditions, and the intermediate species identified by CD and fluorescence spectroscopy is likely a partially unfolded dimer (Fig. 7). As subunit dissociation did not occur until high concentrations of denaturant were added, extraordinary stability comes from both subunit folding and dimer and tetramer assembly. The loss of some secondary, tertiary, and quaternary structure in the first transition also emphasizes the role of cooperativity in contributing to the remarkable stability of *P. furiosus* β-glucosidase. The similarity of the unfolding mechanisms of *P. furiosus* β-glucosidase and *S. solfataricus* β-glycosidase identified using different biophysical methods (Catanzano et al. 1998) shows that unfolding through a dimeric intermediate is not unique for very stable tetrameric proteins. In addition, the high percentage of intermediate seen during denaturation (up to 85% of the total protein) across a relatively broad range of urea concentrations points to the stability of the dimeric intermediate, signifying that even if this is not the only unfolding mechanism occurring, it is predominant.

In agreement with our findings, thermodynamic characterizations of other proteins from thermophiles have shown an increase in the appearance of intermediates in thermophilic proteins (D'Amico et al. 2003). While we were unable to study the thermal denaturation of this β-glucosidase due to irreversible aggregation, previous studies of the thermostabile α-amylase from *Bacillus amyloliquefaciens* (BAA) showed unfolding through an intermediate species whether temperature or GdnHCl was used (Feller et al. 1999; D'Amico et al. 2003). The finding that chemical denaturants interfere with the activity assay for β-glucosidase supports the value of thermodynamic analysis as a tool for understanding the stability of proteins from extremophiles.

Conclusions

We have established an efficient purification protocol for the homo-tetrameric *P. furiosus* β-glucosidase after recombinant expression and secretion by *Saccharomyces cerevisiae*. The thermodynamic unfolding parameters as measured by CD and fluorescence spectroscopy have shown this enzyme to be one of the most stable ever studied, and that unfolding occurs through a stable dimeric intermediate. In the first transition the tetramer dissociates to a dimer, which retains some but not all of its secondary structure. In the second transition the dimer undergoes dissociation and loss of secondary and tertiary structure, yielding an unfolded monomer. To overcome obstacles associated with characterizing oligomeric states of extremely stable proteins at high temperatures, a high temperature native gel electrophoresis technique was developed to visualize the stable dimeric intermediate. These studies provide a platform from which we can assess which features endow *P. furiosus* β-glucosidase with its remarkable stability and should be applicable to the study of stability of β-glucosidase mutations or other hyperthermophilic proteins.

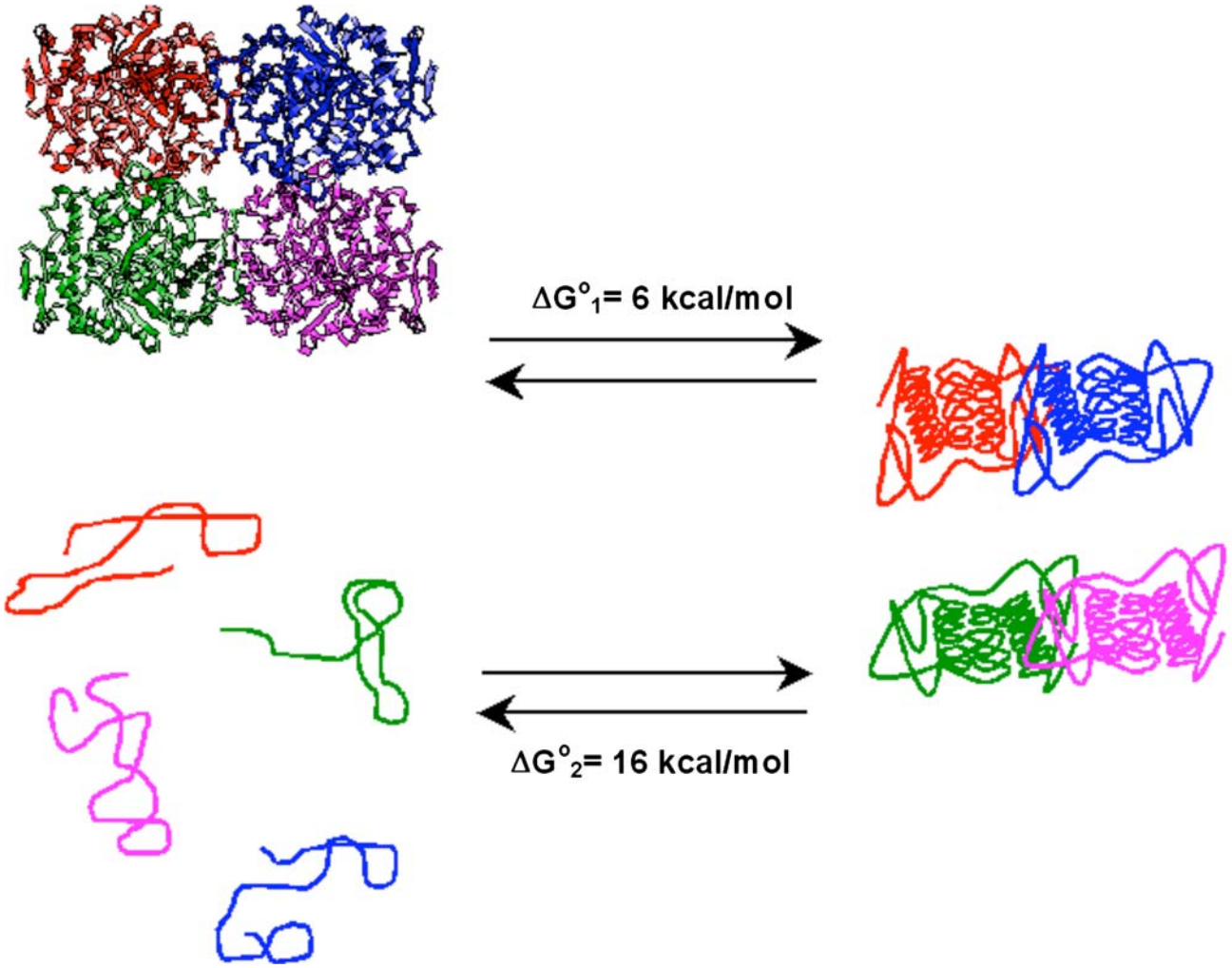

Fig. 7 Model of β-glucosidase unfolding pathway including transitions from tetramer to partially folded dimer to unfolded monomer

Materials and methods

Expression and purification of *P. furiosus* β-glucosidase

β-Glucosidase from *P. furiosus* was expressed in *S. cerevisiae* strain JSIY-017 as described previously (Smith and Robinson 2002). Cultures were grown to saturation in SD-complete media in 250 ml culture flasks at 30°C and 275 rpm. Approximately 10 OD_{600} equivalents were isolated by centrifugation at 2,500*g* for 10 min. Supernatant was decanted, and the cell pellets were resuspended to a final volume of 3 l in YPG expression media. Cultures were allowed to express for 24 h at 37°C and 175 rpm before supernatant containing secreted β-glucosidase was collected by centrifugation at 2,500*g* for 15 min followed by decanting from cell pellet. β-glucosidase production was verified by colorimetric enzymatic activity assay at 90°C (Wood 1988). Residual cellular components were removed by filtration using 0.2 μm cross flow membranes (Sartorius, VivaScience, Göttingen, Germany). The supernatant was then concentrated using 100,000 MWCO cross flow membranes (Sartorius, VivaScience, Göttingen, Germany) to retain β-glucosidase, washed with 2 l of 50 mM Tris, 100 mM NaCl buffer (pH 6.5), and finally concentrated to approximately 100 ml. The sample was separated on DEAE-Sepharose (GE-Amersham Biosciences, Piscataway, NJ, USA) and eluted with a linear gradient of 0.1–1 M NaCl, 50 mM Tris buffer (pH 6.5). The active fractions of the eluted solutions were determined by colorimetric assay and SDS-PAGE and then concentrated and applied to a gel filtration column (Superdex 200 10/30, GE-Amersham Biosciences, Piscataway, NJ, USA) and separated using a 50 mM sodium phosphate buffer (pH 6.5). Purity was greater than 95% as determined by SDS-PAGE and Coomassie staining. Protein concentration was determined spectrophotometrically from the absorbance at 280 nm at pH 6.5 using a cell with a light path length of 1 cm and a molar extinction coefficient ε_{280} of 128 280 M^{-1} cm^{-1}, determined by amino acid analysis (Purdue University, hydrolysis followed by amino acid analysis with a Beckman 166 HPLC system). Protein was

stored at 4°C at 6–10 μM. These protein concentrations, and all the following molar protein concentration reports in the following paper refer to the monomer unit of the protein. A miniDAWN laser photometer (Wyatt Technology Corp., Santa Barbara, CA, USA) was used to determine the oligomeric association at several different protein concentrations ranging from approximately 2–5 μM in 20 mM sodium phosphate buffer. Data were collected at room temperature.

Unfolding recorded by intrinsic fluorescence

Fluorescence was recorded using an ISS PC-1 spectrofluorimeter (Champaign, IL, USA) at an excitation wavelength of 280 and 2 nm band pass, and at emission wavelengths from 300 to 460 nm and 1 nm band pass. To minimize light scattering, excitation polarization was set to 90°, and emission polarization was set to 0° (Ladokhin et al. 2000).

Urea and GdnHCl-induced denaturation was monitored by intrinsic tryptophan fluorescence to construct the unfolding curves and fit thermodynamic parameters (Pace 1986; Eftink 1994). Denatured protein was prepared from the native protein solution diluted in 50 mM sodium phosphate (Sigma, St Louis, MO, USA), pH 6.5, 0M or 8M urea or 6M GdnHCl (ICN/MP Ultrapure, Irvine, CA, USA) stock solutions. Urea stock solutions were deionized with AG 501-X8 Resin (Bio-Rad, Hercules, CA, USA) to remove isocyanic acid. Temperature was maintained at 90°C using a water bath. To minimize effects due to evaporation, solutions for each denaturant concentration were made separately and recorded using a 1 cm sealed quartz cuvette. Equilibrium was reached after incubation for 20 min at 90°C. Samples were stirred constantly throughout incubation and during data collection. The steady-state fluorescence emission spectra for denaturation with urea were recorded at protein concentrations of 0.46, 1.84, and 3.68 μM and corrected for background signal from buffer alone. Denaturation with GdnHCl was completed at a protein concentration of 1.84 μM to assure a similar unfolding profile was seen and any possible contribution due to cyanate formation was negligible. To eliminate the possibility of inner filter effects on the signal at these protein concentrations, wavelength emission scans at an excitation of 260 nm, where the absorbance is less than 0.1, were compared and did not qualitatively impact the results. Fluorescence spectral centers of mass (intensity-weighted average emission wavenumber, ν_{avg}) were calculated with software provided by ISS Inc. as:

$$\upsilon_{avg} = \frac{\sum \upsilon I(\upsilon)}{\sum I(\upsilon)} \quad (1)$$

and then converted to wavelength ($\lambda = 1/\nu$) for ease of comparison. The spectral centers of mass of the fluorescence emission spectra were plotted versus urea concentration. Results are an average of at least three replicates. The spectroscopic data were fit by measuring the change in center of mass or ellipticity determined experimentally as a linear combination of each species performing a nonlinear least-squares regression using the Levenberg–Marquardt (Marquardt 1963) algorithm in MATLAB:

$$Y = f_N Y_N + f_I Y_I + f_U Y_U \quad (2)$$

where Y designates the spectroscopic signal and *f* designates the fraction of native (N), intermediate (I), and unfolded (U) pure species denoted in the subscripts.

To test reversibility, two solutions, a 1.84 μM protein, 0 M urea, 50 mM sodium phosphate buffer, pH 6.5, and a 1.84 μM protein, 8 M urea, 50 mM sodium phosphate buffer, pH 6.5, were heated to 90°C. Appropriate volumes of each solution to achieve the desired denaturant concentration were mixed and the fluorescence spectra were collected after equilibration for 20 min as described in the unfolding process. New solutions were made at each point, as dilution of the same sample was not possible due to evaporation.

Unfolding recorded by far-UV circular dichroism

CD spectra were recorded using a Jasco Model J-810 circular dichroism spectrophotometer (Easton, MD, USA) at 90°C. A 0.1-cm cell path length was used with a protein concentration of 1.84 μM. Samples were prepared as in fluorescence spectroscopy description above. To construct the denaturation curve, at each urea concentration ellipticity was monitored at 225 nm for 20 min, mixed to insure uniformity of the solution, and then the full spectrum was measured for the unfolding data. In the far-UV region, baseline spectra at 0 and 7 M urea were recorded between 190 and 260 nm with sampling points every 1 nm, a time constant of 1 s, and 1 nm bandwidth. A minimum of three kinetic traces were recorded, and baseline buffer spectra were subtracted at each urea concentration.

Activity assay with increasing urea concentration

Enzymatic colorimetric assay was carried out at 90°C using a thermostated spectrophotometer (Model DU600, Beckman, Fullerton, CA, USA) as described previously (Smith and Robinson 2002). Volumes of two solutions, 100 mM sodium acetate, pH 5.5 and 100 mM sodium acetate, 8 M urea (or 6 M GdnHCl), pH 5.5 were mixed to the desired urea concentration and heated to 90°C before adding *p*-NPG and protein. Baseline buffer spectra were subtracted at each urea concentration.

Native PAGE and Ferguson plot analysis

Although analytical ultracentrifugation, size exclusion chromatography, and light scattering are valuable tools to identify oligomeric states (Barry and Matthews 1999;

Ghosh and Mandal 2001; Mamat et al. 2002; Ogasahara et al. 2003), it was not tractable to use these methods at high temperatures. Therefore we chose nondenaturing PAGE and Ferguson plot analysis as described previously to determine oligomeric state changes. To construct Ferguson plots, samples were treated under native and denaturing conditions and run in 6, 7, 8, 9, and 10% native polyacrylamide gels. To reduce variation between individual gels, the stacking gel was omitted. Procedures for running gels at 60°C were refined from the protocol of Haeberle (1997). The samples were prepared with two stock solutions of 0.05 M sodium phosphate, pH 6.5, and 0 or 8 M urea. Samples with standard native or SDS running buffers were preheated to 100°C for 15 min before loading and run at 150 V for 4 h at 60°C. Protein bands were detected by silver staining, and migration distances were measured from the top of the gel to the center of the band of interest.

Data analysis and curve fitting

Denaturation data was fit to a three-state model, to determine thermodynamic parameters for the unfolding transitions:

$$N_4 \overset{K_1}{\longleftrightarrow} 2I_2 \overset{K_2}{\longleftrightarrow} 4U \tag{3}$$

$$\Delta G_i = \Delta G_i^{\circ} - m_i[\text{Urea}] = -RT \ln K_i \tag{4}$$

$$\Delta G_{\text{total}}^{\circ} = \Delta G_1^{\circ} + \Delta G_2^{\circ}. \tag{5}$$

The fractional population in each state can be determined by rearrangement and then fit to experimental data using Eq. 2:

$$f_N = \frac{4\text{N}_4}{P_{\text{tot}}} = \frac{4[\text{U}]^4}{P_{\text{tot}}K_1K_2} \tag{6}$$

$$f_I = \frac{2[\text{I}_2]}{P_{\text{tot}}} = \frac{2[\text{U}]^2}{P_{\text{tot}}K_2{}^{1/2}} \tag{7}$$

$$f_U = \frac{[\text{U}]}{P_{\text{tot}}} \tag{8}$$

where P_{tot} is expressed in monomer units:

$$P_{\text{tot}} = 4[\text{N}_4] + 2[\text{I}_2] + [\text{U}] \tag{9}$$

and the concentration of unfolded protein [U] is determined by solution of the equation (Catanzano et al. 1998):

$$[\text{U}]^4 + [\text{U}]^2\left(\frac{K_1K_2^{1/2}}{2}\right) + ([\text{U}] - P_{\text{tot}})\left(\frac{K_1K_2}{4}\right) = 0 \tag{10}$$

We also attempted to fit the data to a two state transition using the model:

$$\text{N}_4 \overset{\text{K}}{\longleftrightarrow} 4\text{U} \tag{11}$$

The error estimates in Table 1 represent a 95% confidence interval on the four nonlinear least squares parameter estimates using the function nlparci in MATLAB.

Acknowledgments The authors thank Dr. Robert M. Kelly (NC State University) for the generous gift of the β-glucosidase gene. We also thank Dr. Jason Smith, Dr. Tzvetana Lazarova, and Dr. Yu-Sung Wu for experimental assistance and helpful discussions, and Dr. Babatunde Ogunnaike and Claudio Gelmi for discussion of statistics and error analysis. This study was supported by NIH T32 GM 08550-09 (SLP), NSF BES99-84312, and the University of Delaware Research Foundation.

References

Adams MW, Kelly RM (1998) Finding and using hyperthermophilic enzymes. Trends Biotechnol 16:329–332

Barry JK, Matthews KS (1999) Thermodynamic analysis of unfolding and dissociation in lactose repressor protein. Biochemistry 38:6520–6528

Bauer MW, Bylina EJ, Swanson RV, Kelly RM (1996) Comparison of a beta-glucosidase and a beta-mannosidase from the hyperthermophilic archaeon *Pyrococcus furiosus*. Purification, characterization, gene cloning, and sequence analysis. J Biol Chem 271: 23749–23755

Bauer MW, Driskill LE, Kelly RM (1998) Glycosyl hydrolases from hyperthermophilic microorganisms. Curr Opin Biotechnol 9:141–145

Benton CB, King J, Clark PL (2002) Characterization of the protrimer intermediate in the folding pathway of the interdigitated beta-helix tailspike protein. Biochemistry 41:5093–5103

Catanzano F, Graziano G, De Paola B, Barone G, D'Auria S, Rossi M, Nucci R (1998) Guanidine-induced denaturation of beta-glycosidase from *Sulfolobus solfataricus* expressed in *Escherichia coli*. Biochemistry 37:14484–14490

Chen H, Chu Z, Zhang Y, Yang S (2006) Over-expression and characterization of the recombinant small heat shock protein from *Pyrococcus furiosus*. Biotechnol Lett 28:1089–1094

D'Amico S, Marx JC, Gerday C, Feller G (2003) Activity–stability relationships in extremophilic enzymes. J Biol Chem 278: 7891–7896

Demirjian DC, Moris-Varas F, Cassidy CS (2001) Enzymes from extremophiles. Curr Opin Chem Biol 5:144–151

Eftink MR (1994) The use of fluorescence methods to monitor unfolding transitions of proteins. Biophys J 66:482–501

Feller G, d'Amico D, Gerday C (1999) Thermodynamic stability of a cold-active alpha-amylase from the Antarctic bacterium *Alteromonas haloplanctis*. Biochemistry 38:4613–4619

Ferguson KA (1964) Starch-gel electrophoresis–application to the classification of pituitary proteins and polypeptides. Metabolism 13 (Suppl):985–1002

Fiala G, Stetter Karl O (1986) *Pyrococcus furiosus* sp. nov. represents a novel genus of marine heterotrophic archaebacteria growing optimally at 100°C. Arch Microbiol 145:56–61

Gerding JJ, Koppers A, Hagel P, Bloemendal H (1971) Cyanate formation in solutions of urea. II. Effect of urea on the eye lens protein-crystallin. Biochim Biophys Acta 243:375–379

Ghosh M, Mandal DK (2001) Analysis of equilibrium dissociation and unfolding in denaturants of soybean agglutinin and two of its derivatives. Int J Biol Macromol 29:273–280

Grimsley JK, Scholtz JM, Pace CN, Wild JR (1997) Organophosphorus hydrolase is a remarkably stable enzyme that unfolds through a homodimeric intermediate. Biochemistry 36:14366–14374

Haeberle JR (1997) High-temperature sodium dodecyl sulfate polyacrylamide gel electrophoresis. Biotechniques 23:638–640

Hames D (1990) One-dimensional polyacrylamide gel electrophoresis. In: Rickwood BD, Ha D (eds) Gel electrophoresis of proteins: a practical approach. Oxford University Press, Oxford, pp 1–147

Hobart SA, Meinhold DW, Osuna R, Colon W (2002) From two-state to three-state: the effect of the P61A mutation on the dynamics and stability of the factor for inversion stimulation results in an altered equilibrium denaturation mechanism. Biochemistry 41:13744–13754

Kaper T, Lebbink JH, Pouwels J, Kopp J, Schulz GE, van der Oost J, de Vos WM (2000) Comparative structural analysis and substrate specificity engineering of the hyperthermostable beta-glucosidase CelB from *Pyrococcus furiosus*. Biochemistry 39:4963–4970

Kengen SW, Luesink EJ, Stams AJ, Zehnder AJ (1993) Purification and characterization of an extremely thermostable beta-glucosidase from the hyperthermophilic archaeon *Pyrococcus furiosus*. Eur J Biochem 213:305–312

Koutsopoulos S, van der Oost J, Norde W (2005) Conformational studies of a hyperthermostable enzyme. FEBS J 272:5484–5496

Ladokhin AS, Jayasinghe, Sajith, White Stephen H. (2000) How to measure and analyze tryptophan fluorescence in membranes properly, and why bother? Anal Biochem 285:235–245

Machielsen R, van der Oost J (2006) Production and characterization of a thermostable L-threonine dehydrogenase from the hyperthermophilic archaeon *Pyrococcus furiosus*. FEBS J 273:2722–2729

Mamat B, Roth A, Grimm C, Ermler U, Tziatzios C, Schubert D, Thauer RK, Shima S (2002) Crystal structures and enzymatic properties of three formyltransferases from archaea: environmental adaptation and evolutionary relationship. Protein Sci 11:2168–2178

Marquardt DW (1963) An algorithm for least squares estimation of non-linear parameters. J Appl Math 11:431–441

Ogasahara K, Ishida M, Yutani K (2003) Stimulated interaction between and subunits of tryptophan synthase from hyperthermophile enhances its thermal stability. J Biol Chem 278:8922–8928

Pace CN (1986) Determination and analysis of urea and guanidine hydrochloride denaturation curves. Methods Enzymol 131:266–280

Pouwels J, Moracci M, Cobucci-Ponzano B, Perugino G, van der Oost J, Kaper T, Lebbink JH, de Vos WM, Ciaramella M, Rossi M (2000) Activity and stability of hyperthermophilic enzymes: a comparative study on two archaeal beta-glycosidases. Extremophiles 4:157–164

Smith JD, Robinson AS (2002) Overexpression of an archaeal protein in yeast: secretion bottleneck at the ER. Biotechnol Bioeng 79:713–723

Tatur J, Hagedoorn PL, Overeijnder ML, Hagen WR (2006) A highly thermostable ferritin from the hyperthermophilic archaeal anaerobe *Pyrococcus furiosus*. Extremophiles 10:139–148

Timm DE, Neet KE (1992) Equilibrium denaturation studies of mouse beta-nerve growth factor. Protein Sci 1:236–244

Voorhorst WG, Eggen RI, Luesink EJ, de Vos WM (1995) Characterization of the celB gene coding for beta-glucosidase from the hyperthermophilic archaeon *Pyrococcus furiosus* and its expression and site-directed mutation in *Escherichia coli*. J Bacteriol 177:7105–7111

Wallecha A, Mishra S (2003) Purification and characterization of two beta-glucosidases from a thermo-tolerant yeast *Pichia etchellsii*. Biochim Biophys Acta 1649:74–84

Wood T, Bhat KM (1988) Biomass. Part A. Cellulose and hemicellulose. In: Wood WA, Kellogg ST (eds) Methods in enzymology. Academic, San Diego, pp 87–112